Electronic Supplementary Information

Charge Transfer versus Molecular Conductance: Molecular Orbital Symmetry Turns Quantum Interference Rules Upside Down

Natalie Gorczak[1], Nicolas Renaud[1], Simge Tarkuç[1,2], Arjan J. Houtepen[1], Rienk Eelkema[1], Laurens D. A. Siebbeles[1], and Ferdinand C. Grozema[1,*]

[1]Department of Chemical Engineering, Delft University of Technology, Delft, The Netherlands
[2] Department of Biomedical Engineering, Near East University, TRNC, Mersin 10 Turkey

E-mail: f.c.grozema@tudelft.nl

Contents:

S.1. General methods and characterization

All reactions were performed under an argon atmosphere. Commercially available compounds were used without further purification. All reactions were monitored by thin-layer chromatography (TLC) being performed on silica gel 60-F254 (Merck) plates and detected under UV lamp. Column chromatography was carried out on silica gel 60 (Aldrich).

^{1}H NMR and ^{13}C NMR spectra were performed in the appropriate deuterated solvents with tetramethylsilane as internal standard on a Bruker Advance spectrometer at 400 MHz (^{1}H) and 100 MHz (^{13}C); chemical shifts (δ) are reported in parts per million.

1,4-di(thiophen-2-yl)butane-1,4-dione (S1)[1], 9-(tridecan-7-yl)-1H-isochromeno[6',5',4':10,5,6]anthra[2,1,9-def]isoquinoline-1,3,8,10(9H)-tetraone (S8) [2,3], 2-(4-(2,5-di(thiophen-2-yl)-1H-pyrrol-1-yl)phenyl)-9-(tridecan-7-yl)anthra[2,1,9-def:6,5,10-d'e'f']diisoquinoline-1,3,8,10(2H,9H)-tetraone (**1**)[4], 2-(4'-(2,5-di(thiophen-2-yl)-1H-pyrrol-1-yl)-[1,1'-biphenyl]-4-yl)-9-(tridecan-7-yl)anthra[2,1,9-def:6,5,10-d'e'f']diiso- quinoline -1,3,8,10(2H,9H)-tetraone (**2pp**)[4] and 2-(4''-(2,5-di(thiophen-2-yl)-1H-pyrrol-1-yl)-[1,1':4',1''-terphenyl]-4-yl)-9-(tridecan-7-yl)anthra[2,1,9-def:6,5,10-d'e'f']diisoquinoline-1,3,8,10(2H,9H)-tetraone (**3**)[4] were synthesized according to the methods described in the literature.

S.2. Experimental details for synthesis

S.2.1. Synthesis of 1-(3-bromophenyl)-2,5-di(thiophen-2-yl)-1H-pyrrole (S3)[5]

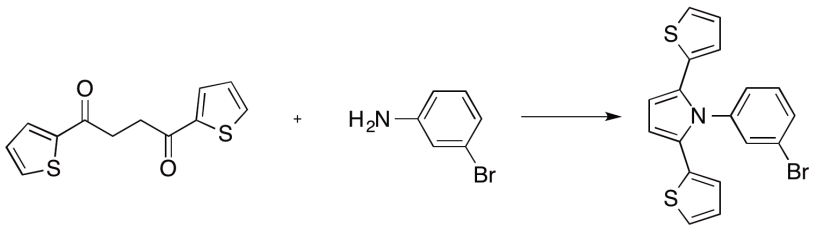

S1 S2 S3

To a 50 mL round bottom flask equipped with a Dean-Stark trap, a reflux condenser and an argon inlet, 1.00 g of 1,4-di(thiophen-2-yl)butane-1,4-dione (**S1**) (4.00 mmol,1.0 equiv), 1.03 g of 3-bromoaniline (**S2**)(6.02 mmol, 1.5 equiv), 0.23 mL of acetic acid (4.00 mmol, 1.0 equiv) and 20 mL of toluene were added. The resulting mixture was refluxed at 111^{o}C for 72 h under argon. After removing the solvent, the crude product was purified by column chromatography in 50 % petroleumether in dichloromethane. The targeted compound was obtained as a yellow solid (603 mg, 39% yield): ^{1}H-NMR (400 MHz, DMSO-d_6) δ 7.76 (d, J = 8.0 Hz, 1H), 7.64 (t, J = 1.9 Hz, 1H), 7.46 (t, J = 7.9 Hz, 1H), 7.40 (d, J = 8.0 Hz, 1H), 7.34 (d, J = 5.1 Hz, 2H), 6.92 (t, J = 4.3 Hz, 2H), 6.72 (d, J = 3.6 Hz, 2H), 6.58 (s, 2H).

S.2.2. Synthesis of S5

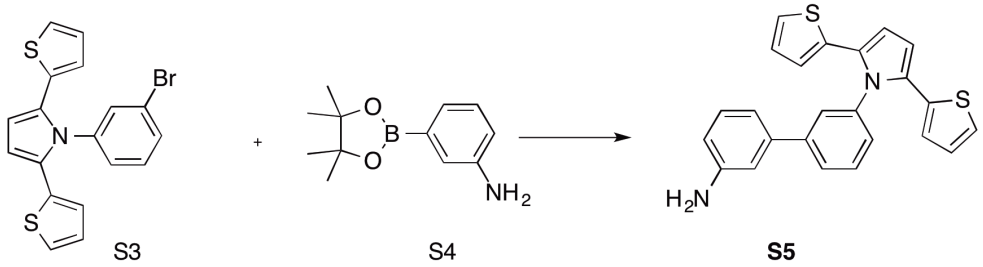

S3 S4 **S5**

To a solution of 200 mg of 1-(3-bromophenyl)-2,5-di(thiophen-2-yl)-1*H*-pyrrole (**S3**) (0.52 mmol, 0.66 equiv) in 15 mL of toluene was added 34 mg of tetrakis(triphenylphosphine) palladium (0.030 mmol, 0.038 equiv) and the mixture was degassed by repeating the freeze-vacuum-thaw cycle three times. Then the flask was filled with argon and stirred at room temperature for 30 min. A degassed solution of Na_2CO_3 (1.54 mmol, 163 mg, 1.97 equiv) in 0.77 mL of water was added into the reaction mixture via a cannula. 3-aminophenylboronicacid pinacolester (0.78 mmol, 171mg, 1.0 equiv) (**S4**) was dissolved into 6 mL of EtOH and degassed. The resulting solution was added to the reaction mixture under argon via a cannula. The reaction mixture was refluxed for 24 h under argon. The mixture was cooled to room temperature and the solvent was removed under reduced pressure. The residue was dissolved in

methylene chloride and extracted with water. The organic layer was dried over $MgSO_4$ and evaporated to dryness. The crude product was purified on a silica gel column eluted with petroleum ether: ethyl acetate (2:1, v/v). Evaporating of the eluting solvent afforded **S5** as a yellow solid (88 mg, 43% yield): ^{1}H-NMR (400 MHz, $CDCl_3$) δ 7.74 - 7.67 (m, 1H), 7.60 (d, *J* = 2.0 Hz, 1H), 7.48 (t, *J* = 7.8 Hz, 1H), 7.32 - 7.26 (m, 1H), 7.23 (t, *J* = 7.8 Hz, 1H), 7.08 (dd, *J* = 5.1, 1.1 Hz, 2H), 7.00-6.94 (m, 1H), 6.85 (dd, *J* = 5.1, 3.6 Hz, 3H), 6.68 (ddd, *J* = 8.0, 2.3, 1.0 Hz, 1H), 6.64 (dd, *J* = 3.7, 1.1 Hz, 2H), 6.62 (s, 2H), 3.72 (s, 2H).

S.2.3. Synthesis of S7

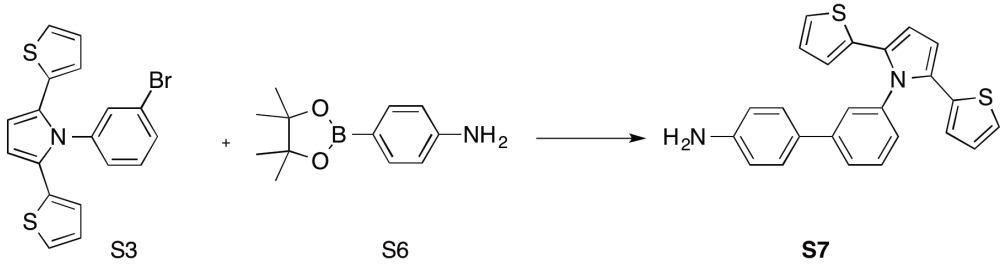

S3 S6 **S7**

The target compound was prepared on a 0.46 mmol scale according to the procedure for compound S5 with the following modifications: 4-aminophenylboronicacid pinacolester (100 mg, 0.46 mmol, 1equiv) (**S6**) was used instead of 3-aminophenylboronicacid pinacolester. The crude product was purified by column chromatography (silica gel; dichloromethane/ petroleum ether = 3:1, v/v) to give **S7** as a pale yellow solid.

^{1}H NMR (400 MHz, Chloroform-*d*) δ 7.66 (dt, *J* = 7.9, 1.4 Hz, 1H), 7.53 (t, *J* = 2.0 Hz, 1H), 7.44 (t, *J* = 7.8 Hz, 1H), 7.39 - 7.36 (m, 2H), 7.20 (ddd, *J* = 7.8, 2.1, 1.1 Hz, 1H), 7.05 (dd, *J* = 5.1, 1.2 Hz, 2H), 6.82 (dd, *J* = 5.1, 3.7 Hz, 2H), 6.76 - 6.72 (m, 2H), 6.61 (dd, *J* = 3.7, 1.2 Hz, 2H), 6.57 (s, 2H), 3.76 (s, 2H).

S.2.4. Synthesis of compound 2mm and 2mp

*2-(3'-(2,5-di(thiophen-2-yl)-1H-pyrrol-1-yl)-[1,1'-biphenyl]-3-yl)-9-(tridecan-7-yl)anthrax[2,1,9-def:6,5,10-d'e'f']diisoquinoline-1,3,8,10(2H,9H)-tetraone (**2mm**).*

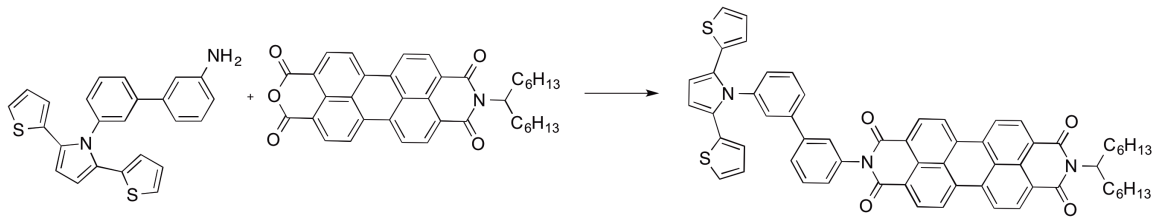

S6 S8 **2mm**

81 mg of S6 (0.203 mmol, 1.0 equiv), 47 mg of 9-(tridecan-7-yl)-1H-isochromeno[6',5',4':10,5,6]anthra[2,1,9-def]isoquinoline-1,3,8,10(9H)-tetraone (0.081 mmol, 0.4 equiv), 14 mg of $Zn(O_2CCH_3)_2.2H_2O$ (0.064 mmol) and 4.5 g of imidazole (0.068 mol) were added to 100 mL round-bottom flask. The reaction mixture was heated to 155^oC for 5 h under an argon atmosphere. The reaction mixture was cooled and 40 mL of chloroform was added to the flask. The resulting mixture was stirred for 15 min and then passed through a silica plug with $CHCl_3$. The eluent was removed under reduced pressure. Purification by column chromatography in 20 % petroleumether in chloroform yielded the product, **2mm** as a red solid (33 mg, 43% yield). ^{1}H NMR (400 MHz, $CDCl_3$): δ 8.81 -8.65 (m, 8H), 8.23 (d, J = 7.9 Hz, 1H), 8.05 (s, 1H), 7.78 (d, J = 8.2 Hz, 1H), 7.66 (dd, J = 7.2, 4.5 Hz, 2H), 7.52 (dd, J = 16.5, 9.2 Hz, 2H), 7.36 (d, J = 7.2 Hz, 1H), 7.05 (d, J = 5.2 Hz, 2H), 6.82 (t, J = 4.4 Hz, 2H), 6.60 (d, J = 3.8 Hz, 2H), 6.56 (s, 2H), 5.20 (m, J = 5.8 Hz, 1H), 2.21-2.31 (m, 2H), 1.90-1.82 (m, 2H), 1.43-1.17 (m, 16H), 0.84 (t, *J* = 6.7 Hz, 6H). ^{13}C-NMR (100MHz, $CDCl_3$): 164.46, 135.12, 133.59, 131.24, 129.11, 128.75, 128.13, 128.22, 127.55, 127.15, 125.89, 124.01, 123.95, 123.87, 123.07, 122.65, 122.17, 121.83, 120.15, 117.16, 109.54, 99.87, 60.59, 31.77, 31.15, 27.95, 25.45, 22.10, 13.57. In ^{13}C-NMR spectrum, 21 aromatic peaks were observed instead of 30

aromatic peaks. 9 aromatic peaks are missing due to overlap of some aromatic carbon signals.

*2-(3'-(2,5-di(thiophen-2-yl)-1H-pyrrol-1-yl)-[1,1'-biphenyl]-4-yl)-9-(tridecan-7-yl)anthra[2,1,9-def:6,5,10-d'e'f']diisoquinoline-1,3,8,10(2H,9H)-tetraone(**2mp**)*

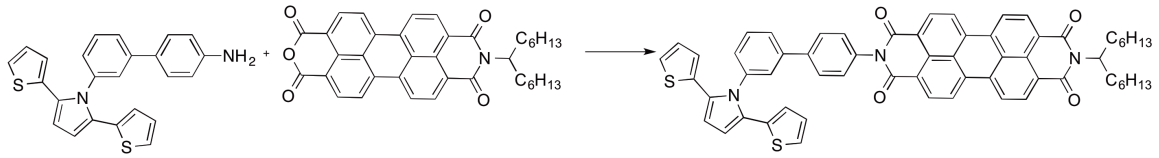

S7 S8 **2mp**

The target compound was prepared on a 0.251 mmol scale according to the procedure for compound **2mm** with the following modifications: **S7** was used instead of **S5**. Column chromatography in 17% petroleumether in chloroform yielded the product as a red solid (43 mg, 45% yield). ^{1}H NMR (400 MHz, Chloroform-*d*) δ 8.75 (d, *J* = 8.0 Hz, 2H), 8.65 (dd, *J* = 8.2, 1.9 Hz, 6H), 7.83-7.75 (m, 2H), 7.74 (s, 1H), 7.67 (d, *J* = 2.0 Hz, 1H), 7.53 (t, *J* = 7.8 Hz, 1H), 7.44 (d, *J* = 8.2 Hz, 2H), 7.32 (dd, *J* = 7.9, 1.9 Hz, 1H), 7.10 (dd, *J* = 5.1, 1.1 Hz, 2H), 6.86 (dd, *J* = 5.1, 3.6 Hz, 2H), 6.64 (dd, *J* = 3.6, 1.1 Hz, 2H), 6.59 (s, 2H), 5.21 (m,1H), 2.44-2.05 (m, 2H), 2.05-1.73 (m, 2H), 1.51-1.11 (m, 16H), 0.84 (t, *J* = 6.7 Hz, 6H). ^{13}C-NMR (100MHz, $CDCl_3$): 163.06, 134.72, 133.65, 131.42, 129.61, 129.18, 128.62, 128.25, 127.68, 127.26, 126.48, 124.12, 124.05, 123.73, 122.87, 122.78, 122.57, 116.61, 109.45, 99.99, 61.67, 31.88, 31.28, 28.73, 26.46, 22.17, 13.57. In ^{13}C-NMR spectrum, 20 aromatic peaks were observed instead of 30 aromatic peaks. 10 aromatic peaks are missing due to overlap of some aromatic carbon signals.

S.3. Experimental methodology

S.3.1. Steady-state and transient absorption spectroscopy

The steady-state absorption spectroscopy measurements were performed on a Perkin-Elmer Lambda 40 spectrophotometer using toluene of spectroscopic grade.

Pump-probe transient absorption measurements were performed using a tunable Yb:KGW laser system comprising a Yb:KGW laser (1028 nm) operating at 5 kHz with a

pulse duration of 200 fs (PHAROS-SP-06-200, Light Conversion) and an optical parametric amplifier (ORPHEUS-PO15F5HNP1, Light Conversion). White light continuum pulses, generated by focusing the fundamental on a sapphire crystal, were used as probe. A transient absorption spectrometer (HELIOS, Ultrafast Systems) was employed for data acquisition in a spectral window of 490-910 nm and a time window of 3.3 ns. The samples were placed in 2 mm path length quartz cuvettes using toluene of spectroscopic grade as solvent. In order to prevent aggregation of the compounds the absorbance at 527 nm was kept at 0.1. The samples were excited at 350 nm (excitation of SNS) and 527 nm (excitation of PDI) with pulses of 0.2 μJ and a 200 μm spotsize in quasi parallel pump-probe geometry. During the experiments the samples were stirred continuously with a magnetic stirrer.

The two-dimensional data was analyzed with global and target analysis utilizing the open source software Glotaran[6], a graphical user interface for the R package TIMP[7]. TIMP is based on spectrotemporal parameterization assuming that the time dependent spectra are linear combinations of difference absorption spectra of various species with their respective population profiles[8]. A parameterised Gaussian instrument response function accounting for dispersion and the coherent artifact were taken into account. To model the photophysical processes after excitation at 527 nm, target analysis was applied with the sequential kinetic schemes depicted in Figure 4(a). The photophysical processes after excitation at 350 nm were modeled with the compartmental kinetic scheme depicted in Figure 5(a). Applying a correct scheme yields transient absorption (ΔOD) spectra of the excited or radical ion states involved in the photophysical processes together with their population profiles. The quality of the fits was therefore not only examined on the basis of the residuals but also the meaningfulness of the ΔOD spectra of all excited states (hot PDI*, PDI*, and SNS*) and the radical anion state ($PDI^{-\bullet}$). In particular, the ΔOD spectra obtained from the analysis of each dataset of the DBA systems should be comparable to each other and to that of the neat PDI and SNS. Small deviations are possible due to different chemical surrounding that can induce slight shifts of transition energies or change in the oscillator strength.

S.4. Structures of the DBA systems used in the calculations

*S.4.1. Coordinates of **1***

H	0.00000000	0.00000000	15.21066800
H	3.34151100	0.00000000	11.98795200
C	2.41957600	0.00000000	11.42322000
C	1.24475600	0.00000000	13.59019200
C	1.22912000	0.00000000	12.10511300
C	1.24906100	0.00000000	9.29356700
C	0.00000000	0.00000000	11.40310300
C	2.42550400	0.00000000	10.02306000
C	0.00000000	0.00000000	9.98570000
C	-1.22912000	0.00000000	12.10511300
H	3.37974800	0.00000000	9.52052300
C	-1.24829800	0.00000000	7.81902600
C	-2.41957600	0.00000000	11.42322000
C	-1.24475600	0.00000000	13.59019200
H	-3.34151100	0.00000000	11.98795200
C	-2.42550400	0.00000000	10.02306000
H	-3.37974800	0.00000000	9.52052300
C	-1.24906100	0.00000000	9.29356700
O	2.25790300	0.00000000	14.25171000
O	-2.25790300	0.00000000	14.25171000
N	0.00000000	0.00000000	14.19759800
N	0.00000000	0.00000000	2.86309600
H	-3.33411100	0.00000000	5.11872300
C	-2.41238700	0.00000000	5.68274400
C	-1.23986400	0.00000000	3.51160100
C	-1.22026900	0.00000000	5.00235700
C	0.00000000	0.00000000	5.71177200
C	-2.42139400	0.00000000	7.08414300
C	0.00000000	0.00000000	7.12883000
C	1.22026900	0.00000000	5.00235700
H	-3.37772300	0.00000000	7.58341500
C	2.41238700	0.00000000	5.68274400
C	1.23986400	0.00000000	3.51160100
H	3.33411100	0.00000000	5.11872300
C	2.42139400	0.00000000	7.08414300
H	3.37772300	0.00000000	7.58341500
C	1.24829800	0.00000000	7.81902600
O	-2.27119900	0.00000000	2.88449900
O	2.27119900	0.00000000	2.88449900
C	0.00000000	0.00000000	1.41909600
C	0.50984200	1.09335424	0.72256600

C	0.50986229	1.09339774	-0.67054300
C	0.00000000	0.00000000	-1.36712300
C	-0.50986229	-1.09339774	-0.67054300
C	-0.50984200	-1.09335424	0.72256600
H	0.90609178	1.94311038	1.26389900
H	0.90608840	1.94310313	-1.21203500
H	-0.90608840	-1.94310313	-1.21203500
H	-0.90609178	-1.94311038	1.26389900
H	5.71126667	1.93539801	-3.20155700
C	1.08529431	0.29080236	-3.61156500
C	0.68087449	0.18307831	-4.92165900
N	0.00000000	0.00000000	-2.79612300
H	1.32784232	0.31724424	-5.77197900
C	-0.68087449	-0.18307831	-4.92165900
H	-1.32784232	-0.31724424	-5.77197900
C	-1.08529431	-0.29080236	-3.61156500
C	-2.44620286	-0.57810912	-3.15627200
H	-2.79883497	0.84912351	-1.58208700
C	-3.19078394	0.05127794	-2.19812300
C	-4.52963415	-0.43122188	-2.13088700
H	-5.27326486	-0.03967051	-1.45136700
C	-4.77958313	-1.41962459	-3.03466600
S	-3.38167023	-1.80787867	-3.98384100
H	-5.71126667	-1.93539801	-3.20155700
C	2.44620286	0.57810912	-3.15627200
C	4.77958313	1.41962459	-3.03466600
H	5.27326486	0.03967051	-1.45136700
C	4.52963415	0.43122188	-2.13088700
C	3.19078394	-0.05127794	-2.19812300
H	2.79883497	-0.84912351	-1.58208700
S	3.38167023	1.80787867	-3.98384100

*S.4.2. Coordinates of **2mm***

H	9.30988953	-8.83806940	1.17527019
H	7.02430183	-5.94216981	3.99332779
C	6.41402494	-5.99207318	3.10228450
C	8.10003688	-7.54292760	2.19223834
C	6.83036378	-6.78355397	2.06190780
C	4.43351721	-5.32759302	1.86067968
C	6.06017777	-6.87630409	0.87794626
C	5.21982978	-5.26847932	2.99839506
C	4.85044104	-6.14601792	0.76726454
C	6.48830624	-7.69244507	-0.19637861
H	4.92370090	-4.65674306	3.83577877

C	2.82751303	-5.49122239	-0.54868728
C	5.74066984	-7.78126469	-1.34325020
C	7.75362792	-8.46338096	-0.09477640
C	4.54482494	-7.06205438	-1.45803126
H	3.98313504	-7.15594806	-2.37389887
C	4.08591019	-6.25122978	-0.43424472
O	8.80561139	-7.50916708	3.17463223
O	8.17724902	-9.17880709	-0.97385747
N	8.44524625	-8.31610705	1.09616190
N	-1.22861736	-2.47625063	0.21107690
H	0.23260099	-4.87114256	-2.67570036
C	0.84224169	-4.82095088	-1.78490642
C	-0.84764977	-3.26879672	-0.87729614
C	0.42741946	-4.02963153	-0.74288532
C	1.20269397	-3.94396918	0.43352341
C	2.03706589	-5.54632151	-1.68374879
C	2.41213624	-4.67407759	0.54417818
C	0.76701382	-3.12728544	1.49913898
H	2.33011801	-6.15714645	-2.52330286
C	1.51359613	-3.03707538	2.64741978
C	-0.50260223	-2.35196082	1.40073044
H	1.16046631	-2.40568452	3.45012752
C	2.71092693	-3.75578565	2.76512615
H	3.27012032	-3.65943887	3.68265421
C	3.17490771	-4.56814984	1.74483525
O	-1.52638144	-3.32701403	-1.87371115
O	-0.89431886	-1.64754210	2.29920756
H	6.09437713	-8.41309990	-2.14609626
C	-4.82878131	-0.28876594	-0.09386672
C	-3.61445731	0.39827706	0.00203028
C	-4.86088831	-1.67936194	-0.09796372
C	-3.67627531	-2.40468794	-0.00111972
C	-2.46105431	-1.73226094	0.09831828
C	-2.43191531	-0.34169994	0.09745028
H	-5.74865931	0.27428306	-0.19230572
H	-5.80825431	-2.19597094	-0.18351872
H	-3.69988731	-3.48691194	-0.00270672
H	-1.48805831	0.18000106	0.19699728
C	-3.58084231	1.88732906	0.00210628
C	-2.62257331	2.57968906	-0.74505472
C	-2.59150131	3.97020306	-0.74808172
C	-3.51852431	4.69014206	0.00101528
C	-4.47553931	4.01247606	0.75180428
C	-4.50633231	2.62190906	0.74986028

H	-1.91516331	2.02122306	-1.34556672
H	-3.49469231	5.77235806	0.00035728
H	-5.19368131	4.56598406	1.34310628
H	-5.23738831	2.09580906	1.35126728
H	-3.25667290	1.97976706	-6.69158169
C	-1.45792780	4.56924950	-2.90588249
C	-0.40838613	5.37786970	-3.27480226
N	-1.61177073	4.65751584	-1.52895953
H	-0.08724580	5.53373991	-4.29076748
C	0.09940395	5.98181984	-2.10611735
H	0.94423213	6.64391436	-2.01946776
C	-0.64747026	5.53019604	-1.04323400
C	-0.41146027	5.84796088	0.36574923
H	-0.57163360	3.95351197	1.37807756
C	-0.36143855	5.01221166	1.44630447
C	0.02832612	5.67778914	2.64419293
H	0.14582014	5.17800299	3.59522158
C	0.26448469	7.00632943	2.45593595
S	-0.00144088	7.49236311	0.81310615
H	0.58906717	7.72527157	3.19056338
C	-2.31824077	3.81351587	-3.81727552
C	-3.16093326	2.53816851	-5.77455891
H	-5.21330642	2.84344159	-5.18345539
C	-4.16404680	2.99731923	-4.97507487
C	-3.68208736	3.72757434	-3.85066870
H	-4.31660793	4.19367863	-3.10917538
S	-1.59348808	2.96519307	-5.16908347

S.4.3. Coordinates of ***2mp***

H	-3.99986620	-16.20556156	-0.02340759
H	-0.58965090	-13.05659315	0.05420493
C	-1.49882821	-12.47186140	0.03492287
C	-2.72035618	-14.61265786	0.00611979
C	-2.70359097	-13.12759232	0.00795596
C	-2.62233172	-10.31715379	0.01251287
C	-3.91681248	-12.39890658	-0.01782541
C	-1.46236159	-11.07216551	0.03710491
C	-3.88589492	-10.98184234	-0.01574740
C	-5.16065962	-13.07390528	-0.04566518
H	-0.49761054	-10.59058895	0.05865642
C	-5.08633684	-8.78842383	-0.03979979
C	-6.33567436	-12.36617614	-0.07063268
C	-5.20868193	-14.55828786	-0.04818349
H	-7.26948846	-12.91063845	-0.09157062

C	-6.31105810	-10.96622132	-0.06870925
H	-7.25388566	-10.44296409	-0.08878724
C	-5.11926337	-10.26259574	-0.04197822
O	-1.72212151	-15.29614451	0.02724955
O	-6.23577574	-15.19752100	-0.07125291
N	-3.97776829	-15.19273369	-0.02192235
N	-3.73053084	-3.86094067	-0.00530513
H	-7.11225473	-6.04321283	-0.08133841
C	-6.20327282	-6.62722914	-0.06205990
C	-4.98394978	-4.48221251	-0.03330082
C	-4.99688170	-5.97304016	-0.03505895
C	-3.79266850	-6.70893582	-0.00948150
C	-6.24284399	-8.02809649	-0.06431093
C	-3.82357853	-8.12565514	-0.01155901
C	-2.55750661	-6.02634059	0.01817606
H	-7.20960783	-8.50636329	-0.08590313
C	-1.38079781	-6.73260039	0.04318202
C	-2.50540336	-4.53636884	0.02078904
H	-0.44721013	-6.18884430	0.06411432
C	-1.40236357	-8.13386116	0.04132393
H	-0.45738079	-8.65389970	0.06145219
C	-2.59093046	-8.84294854	0.01465801
O	-6.00111448	-3.83273642	-0.05487776
O	-1.46088093	-3.93194068	0.04420475
C	-3.63852666	0.38570784	-0.00004728
C	-4.18336098	-0.31766500	1.07894730
C	-4.21626472	-1.70824793	1.07779353
C	-3.69903313	-2.41728579	-0.00318812
C	-3.15075814	-1.72857949	-1.08202371
C	-3.12356347	-0.33798040	-1.07993837
H	-4.60660773	0.23318575	1.90979963
H	-4.65106587	-2.23739477	1.91604077
H	-2.73890396	-2.27377496	-1.92160164
H	-2.67698351	0.19593292	-1.90966753
C	-3.60758286	1.87481770	0.00031336
C	-3.94072002	2.59594590	-1.15072320
C	-3.91482125	3.98656908	-1.15123015
C	-3.55083681	4.67774904	0.00142578
C	-3.21368261	3.97125918	1.15294311
C	-3.24410060	2.58068346	1.15136060
H	-4.24543449	2.05998758	-2.04113075
H	-3.52923097	5.76001183	0.00198210
H	-2.92154365	4.50227671	2.04983346
H	-2.96073233	2.03202794	2.04107629

H	0.94677460	7.74511475	-2.55397773
C	-3.45681284	5.58757931	-3.02924618
C	-4.16324440	6.06859385	-4.10678301
N	-4.27146321	4.70362929	-2.33473012
H	-3.76478088	6.74544188	-4.84347530
C	-5.44064119	5.47181699	-4.08342149
H	-6.26354109	5.64833584	-4.75520182
C	-5.49314064	4.63804317	-2.99091465
C	-6.66360679	3.87909085	-2.54829822
H	-6.74646212	4.21073017	-0.42166916
C	-7.20193735	3.76752676	-1.29676627
C	-8.42940786	3.04434208	-1.28385476
H	-9.01371246	2.87339198	-0.39087619
C	-8.80170992	2.61598084	-2.52245425
S	-7.65451158	3.06424216	-3.74263155
H	-9.69207300	2.06903058	-2.78704461
C	-2.05908764	5.88960722	-2.71771390
C	0.13971501	7.03067548	-2.54212933
H	1.14201966	5.18429203	-2.05112613
C	0.21853333	5.69529680	-2.28370655
C	-1.04249796	5.03958904	-2.38216495
H	-1.19047944	3.97814224	-2.23685816
S	-1.48126309	7.53499027	-2.89416837

S.4.4. Coordinates of ***2pp***

H	-3.99986620	-16.20556156	-0.02340759
H	-0.58965090	-13.05659315	0.05420493
C	-1.49882821	-12.47186140	0.03492287
C	-2.72035618	-14.61265786	0.00611979
C	-2.70359097	-13.12759232	0.00795596
C	-2.62233172	-10.31715379	0.01251287
C	-3.91681248	-12.39890658	-0.01782541
C	-1.46236159	-11.07216551	0.03710491
C	-3.88589492	-10.98184234	-0.01574740
C	-5.16065962	-13.07390528	-0.04566518
H	-0.49761054	-10.59058895	0.05865642
C	-5.08633684	-8.78842383	-0.03979979
C	-6.33567436	-12.36617614	-0.07063268
C	-5.20868193	-14.55828786	-0.04818349
H	-7.26948846	-12.91063845	-0.09157062
C	-6.31105810	-10.96622132	-0.06870925
H	-7.25388566	-10.44296409	-0.08878724
C	-5.11926337	-10.26259574	-0.04197822
O	-1.72212151	-15.29614451	0.02724955

O	-6.23577574	-15.19752100	-0.07125291
N	-3.97776829	-15.19273369	-0.02192235
N	-3.73053084	-3.86094067	-0.00530513
H	-7.11225473	-6.04321283	-0.08133841
C	-6.20327282	-6.62722914	-0.06205990
C	-4.98394978	-4.48221251	-0.03330082
C	-4.99688170	-5.97304016	-0.03505895
C	-3.79266850	-6.70893582	-0.00948150
C	-6.24284399	-8.02809649	-0.06431093
C	-3.82357853	-8.12565514	-0.01155901
C	-2.55750661	-6.02634059	0.01817606
H	-7.20960783	-8.50636329	-0.08590313
C	-1.38079781	-6.73260039	0.04318202
C	-2.50540336	-4.53636884	0.02078904
H	-0.44721013	-6.18884430	0.06411432
C	-1.40236357	-8.13386116	0.04132393
H	-0.45738079	-8.65389970	0.06145219
C	-2.59093046	-8.84294854	0.01465801
O	-6.00111448	-3.83273642	-0.05487776
O	-1.46088093	-3.93194068	0.04420475
C	-3.63852708	0.38570785	-0.00004699
C	-4.18288310	-0.31767577	1.07918195
C	-4.21578645	-1.70825871	1.07802932
C	-3.69903313	-2.41728579	-0.00318812
C	-3.15123637	-1.72856870	-1.08225974
C	-3.12404167	-0.33796962	-1.08017300
H	-4.60576225	0.23316667	1.91022695
H	-4.65021601	-2.23741394	1.91646390
H	-2.73975366	-2.27375580	-1.92202523
H	-2.67782952	0.19595201	-1.91009467
C	-3.60758409	1.87481773	0.00031434
C	-3.94123138	2.59595683	-1.15056762
C	-3.91533375	3.98658003	-1.15107260
C	-3.55083937	4.67774909	0.00142872
C	-3.21317483	3.97124832	1.15278981
C	-3.24359261	2.58067260	1.15120733
H	-4.24633978	2.06000692	-2.04084533
H	-4.18588920	4.52976535	-2.04745501
H	-2.92063908	4.50225738	2.04955584
H	-2.95983004	2.03200867	2.04079214
H	2.25770058	6.39569447	1.74470379
C	-2.41180696	6.89976844	0.25674195
C	-2.79338858	8.21778931	0.16334696
N	-3.52231769	6.10646424	0.00216429

H	-2.12543578	9.05488632	0.27612817
C	-4.16639887	8.24536378	-0.15683012
H	-4.80040829	9.10856777	-0.26873593
C	-4.60027731	6.94371895	-0.25157386
C	-5.97888603	6.51598097	-0.49320826
H	-6.31471875	4.94744631	0.94426043
C	-6.72087728	5.57211694	0.16035753
C	-8.07625695	5.53215033	-0.27690130
H	-8.81972770	4.86712271	0.13907470
C	-8.34118282	6.44190231	-1.25587857
S	-6.93843676	7.36348702	-1.69041279
H	-9.28615170	6.62794038	-1.73995781
C	-1.05137280	6.41710193	0.49790762
C	1.30606968	6.24801708	1.26045274
H	1.72141184	4.65682989	-0.13613054
C	1.00506642	5.35057137	0.28054503
C	-0.34762929	5.44504995	-0.15664458
H	-0.77837898	4.83789418	-0.94118169
S	-0.05878686	7.22440395	1.69596413

S.4.5. Coordinates of ***3***

H	-4.61280478	-16.10407963	-1.77340304
H	-1.09257260	-13.12697949	-1.22894523
C	-1.97719608	-12.50545203	-1.22335163
C	-3.27645129	-14.57826776	-1.52557758
C	-3.20354564	-13.10335943	-1.36735530
C	-3.01617489	-10.31434957	-1.06485775
C	-4.38595396	-12.32524596	-1.36535157
C	-1.88787155	-11.11625002	-1.07294524
C	-4.30150654	-10.91853847	-1.21345046
C	-5.65201235	-12.94055796	-1.51381472
H	-0.90748073	-10.68070166	-0.96223616
C	-5.41575343	-8.68554305	-1.05562333
C	-6.79710894	-12.18497029	-1.51166334
C	-5.75606567	-14.41339525	-1.67390016
H	-7.74902473	-12.68438406	-1.62711283
C	-6.71959327	-10.79498310	-1.36196332
H	-7.64010282	-10.23304160	-1.36496001
C	-5.50436504	-10.14890684	-1.21369330
O	-2.30674485	-15.30189157	-1.53610929
O	-6.80459724	-15.00282401	-1.80515638
N	-4.55244711	-15.09865411	-1.66483373
N	-3.87714909	-3.84968060	-0.45013086
H	-7.33239252	-5.86747933	-0.89050620

C	-6.44793684	-6.48828718	-0.89603617
C	-5.15072100	-4.41117980	-0.59350007
C	-5.22002162	-5.89198449	-0.75209487
C	-4.04687029	-6.67686091	-0.75541952
C	-6.54040195	-7.87851492	-1.04675879
C	-4.13129715	-8.08322599	-0.90728366
C	-2.78918653	-6.05361361	-0.60669012
H	-7.52267496	-8.31068484	-1.15724218
C	-1.64234483	-6.80781671	-0.60858108
C	-2.68085172	-4.57540435	-0.44576042
H	-0.69068156	-6.30909460	-0.49322036
C	-1.71686755	-8.19923747	-0.75823044
H	-0.79408677	-8.75807668	-0.75475963
C	-2.92908322	-8.85088471	-0.90687869
O	-6.14059359	-3.72050776	-0.58774030
O	-1.61625493	-4.02133642	-0.31710888
C	-3.62128491	0.36344089	0.00546670
C	-4.24426610	-0.42147123	0.98086632
C	-4.32887875	-1.80207846	0.83271639
C	-3.79111705	-2.41657681	-0.29537938
C	-3.16934911	-1.64498431	-1.27360387
C	-3.08586822	-0.26490504	-1.12356664
H	-4.68244526	0.05882827	1.84694511
H	-4.82083184	-2.39653437	1.59175274
H	-2.74035926	-2.11862397	-2.14720653
H	-2.57904549	0.33228384	-1.87148842
C	-3.52824457	1.83740763	0.16544885
C	-3.78080377	2.69251121	-0.91057396
C	-3.69568666	4.06997189	-0.76010424
C	-3.34584021	4.63744081	0.46812983
C	-3.08916621	3.78159927	1.54245494
C	-3.18426757	2.40459093	1.39526476
H	-4.06256480	2.27160921	-1.86753149
H	-3.88426653	4.71655615	-1.60786559
H	-2.97250890	1.75683881	2.23667471
H	-2.83242736	4.20321113	2.50605149
C	-3.25065272	6.11239081	0.62725161
C	-2.18350007	6.68782318	1.32460964
C	-2.09386817	8.06756362	1.47281066
C	-3.07208742	8.89449189	0.92622494
C	-4.13947579	8.33305332	0.22996898
C	-4.22663953	6.95292192	0.08182240
H	-1.41153757	6.04723207	1.73294929
H	-1.25777275	8.49755921	2.00908935

H	-4.90811112	8.96873416	-0.19036146
H	-5.06920919	6.51607569	-0.44004715
H	2.51423098	10.64074417	-1.41324727
C	-1.94346782	11.11674410	0.62997742
C	-2.22794720	12.41830031	0.97134096
N	-2.98178061	10.31235464	1.07968798
H	-1.61281927	13.26394943	0.71422784
C	-3.46696406	12.42434924	1.64456573
H	-3.97461866	13.26608577	2.08431382
C	-3.91702835	11.12613851	1.70454228
C	-5.13018263	10.67089619	2.38492459
H	-4.50765513	8.92580785	3.48334483
C	-5.29979539	9.62283029	3.24595186
C	-6.60615959	9.57693398	3.81265527
H	-6.92043176	8.83421956	4.53213760
C	-7.40763846	10.58658920	3.37168041
S	-6.59929327	11.61490366	2.23370752
H	-8.42654873	10.78851342	3.65970389
C	-0.78785877	10.66849729	-0.14819446
C	1.47422709	10.51148779	-1.16106928
H	0.78690466	9.12193907	-2.66159346
C	0.55851812	9.72767266	-1.79616123
C	-0.73934801	9.81520030	-1.21501662
H	-1.60935006	9.28975319	-1.58472415
S	0.78584967	11.36672809	0.18077104

S.5. Interference in meta-meta biphenyl junction

As mentioned in the text the low conductance observed for the meta-meta junctions is reminiscent from destructive quantum interference. Here, we demonstrate the existence of these interference and illustrate the disappearance of the sharp dip of the transmission coefficient when accounting for non-nearest neighbor couplings. We start with a topological model of the biphenyl where each carbon atom is represented by a single orbital. For simplicity the energy of these orbitals was set to $\varepsilon = 0$. These orbitals are only coupled with their nearest neighbors as represented in Fig. 1. Once again for simplicity this coupling was set to $\alpha = -1$ eV. As represented in this figure, the lead is here coupled directly to two carbon atoms. The magnitude of this coupling was here set to $\Gamma = 0.5$ eV. The transmission of this system, calculated using the Green function approach described in the text and assuming a para-para (2pp) meta-para (2mp) and meta-meta (2mm)

connection to the leads, are shown in Fig. 1. As seen on this figure, a clear interference pattern appears at $E = 0$ in meta-meta configuration, with a perfect cancellation of the transmission coefficient.

As seen in Fig. 1, the graph of the molecule respects the alternating hydrocarbons connection rules, with two types of sites, represented with and without an asterisk respectively. The asterisk atoms are only connected to non-asterisk atoms and inversely. As a consequence, the eigenvalues of this graph respect the conditions: $E_n = -E_{-n}$ and the eigenvectors, labeled $|\varphi_{\pm n}>$, respect the condition: $<k|\varphi_n> = <k|\varphi_{-n}>$ if $|k>$ is the orbital of an asterisk atom and $<k|\varphi_n> = -<k|\varphi_{-n}>$ if $|k>$ is not an asterisk atom. It is easy to demonstrate with these properties that connecting the electrodes on two atoms of the same type, either with or without asterisk, leads to destructive interference. This can be done by computing the Green function between the two electrodes. If the two electrodes are for example connected to the sites $|1>$ and $|11>$ by a coupling γ, the Green function reads:

$$G(E) = \gamma \sum_{n=1}^{N/2} \frac{<1|\varphi_n><\varphi_n|11>}{E - E_n} + \frac{<1|\varphi_{-n}><\varphi_{-n}|11>}{E - E_{-n}} \qquad (1)$$

Since $E_n = -E_{-n}$, $<\varphi_n|1> = <\varphi_{-n}|1>$ and $<\varphi_n|11> = <\varphi_{-n}|11>$, we obtain $G(E{=}0) = 0$, which leads to a cancellation of the transmission coefficient, i.e. a perfect destructive interference (see curve 2mp in Fig. 1). This interference comes from a pair-wise cancellation of the contributions of the different molecular orbitals of the graph, the contribution of $|\varphi_n>$ canceling those of $|\varphi_{-n}>$. However when connecting the electrodes on two atoms of different types one does not expect destructive interference. This is the case of the para-para connection, when atoms $|1>$ and $|12>$ are connected to the leads. There, since $<\varphi_n|12> = -<\varphi_{-n}|12>$, the contribution of $|\varphi_n>$ does not cancel the contribution of $|\varphi_{-n}>$ in $G(E)$, and no interference appears in the transmission coefficient (see curve 2pp in Fig. 1). In this respect, the appearance of destructive interference in the meta-meta connection, e.g. when the electrodes are connected to the atoms $|2>$ and $|11>$, is somehow surprising (see curve 2mm in Fig. 1). A numerical evaluation of $G(E)$ in the meta-meta connection shows that a pair-wise cancellation of the different contribution of $G(E)$ does indeed not occur. Instead, a

global cancellation of all the contributions is responsible for the destructive interference observed in Fig. 1. An in-depth investigation of the symmetry properties required to observe such global cancellation of $G(E)$ would be of interest but is beyond the scope of this article.

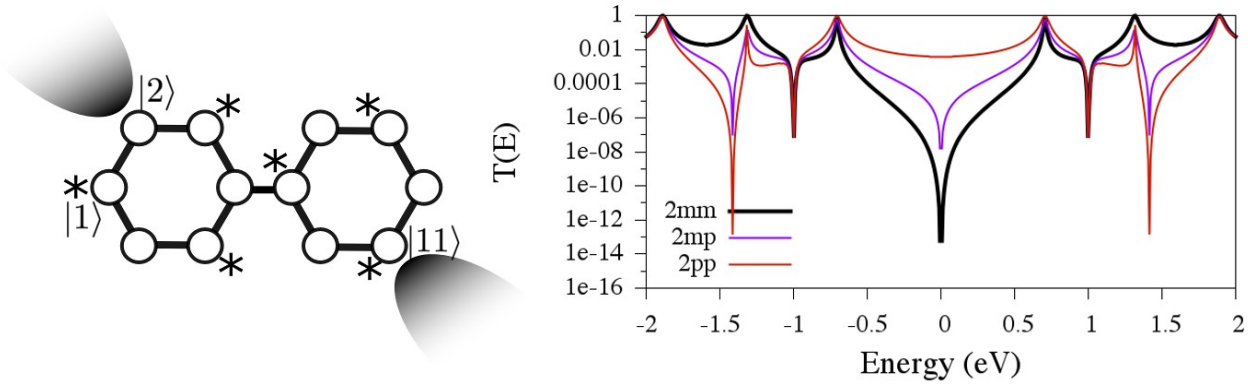

FIG. 1. Left: Topological graph representing a biphenyl molecule connected in meta-meta. Right: Transmission of a topological biphenyl graph showing a clear destructive interference at $E = 0$ in meta-meta (2mm) and meta-para (2mp) configuration but not in para-para (2pp) configuration.

The destructive interference observed in the meta-meta connection persists when using a more elaborate model for the molecule. We consider here an extended Huckel model for the molecule where each carbon atom is represented by one $2s$ orbital and three $2p$ orbitals ($2p_x$,$2p_y$,$2p_z$). Similarly each hydrogen atom is represented by its $1s$ orbital. We used standard values for the Slater orbitals leading in particular to $E_{C_{p_{x/y/z}}} = -11.4$ eV and $\alpha = -4.8082$ eV, where α is the coupling between the p_z orbitals of two neighboring carbon atoms separated by a distance of 1.41 angstroms. We assume here that the coupling between the molecule and the leads is made through the p_z orbitals of two carbon atoms highlighted in Fig. 2. As previously, this coupling was set to $\Gamma = 0.5$ eV. The Fermi energy of the leads was set to -10.62 eV, i.e. the energy of the 6s orbitals of gold in the Hückel model. We then consider two cases; one where the full extended Hückel Hamiltonian was used and one where the interactions between the two phenyls were limited to the connecting atoms. In the latter case, the transmission coefficient (thick dashed line in Fig. 2) shows a sharp interference dip. However, when accounting for all the interactions between the two phenyl rings, this sharp feature disappears (thick

plain line). This disappearance of the interference feature comes from the possibility for the electrons to directly propagate from one phenyl to another via through-space couplings. These additional pathways bypass the through-bond coupling along the phenyl rings that leads to sharp destructive interference. However these pathways are mediated by weak long-range couplings leading therefore to a weak transmission. Therefore, even when accounting for the through-space couplings, the value of the transmission coefficient in meta-meta configuration is much lower than in the para-para configuration (thin plain line).

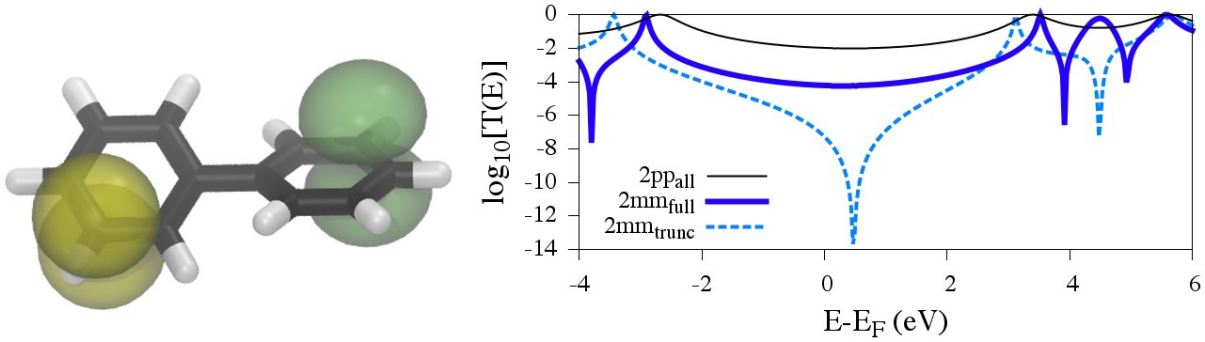

FIG. 2. Left: Representation of the biphenyl molecule showing the two $2p_z$ orbitals connected to the electrodes. Right: Transmission coefficient obtained using an extended Huckel model for the electronic structure. The meta-meta connection shows a much lower transmission than the para-para one. This is due to destructive quantum interference that clearly appears when the couplings between the two phenyls are limited to the coupling between the connecting atoms ($2\mathrm{mm}_{trunc}$)

The same analysis can be done at the DFT level of theory. Fig. 3 shows the transmission coefficient of the molecule denoted **S2mm** in the main text and obtained at the DFT level of theory. A wide-band limit approach was used here as well and only the $2p_z$ orbitals of the sulfur atoms were connected to electrodes via a coupling $\Gamma = 0.5$ eV. As previously two situations are represented. First the full DFT Hamiltonian was used to compute the transmission (thick black line). This corresponds to the curve shown in the main text in Fig. 2. As explained in the main text, this curve does not show a sharp destructive interference pattern but is much lower than the one obtained in a para-para configuration. When limiting the interactions between the two phenyls to interactions between the two

connecting atoms, two sharp interference dips are obtained. These two dips come from the two interference of the two distinct phenyl rings that occur at different energies due to small distortion of the rings. If the two rings were identical, the two interference dips would merge in one single dip. This result clearly shows that the low values of the transmission coefficient obtained for the meta-meta configuration comes from destructive quantum interference. The sharp features characteristic of destructive interference are however washed away by the through-space coupling between the two phenyls that leads to a weak transmission when the full Hamiltonian is considered in the calculation.

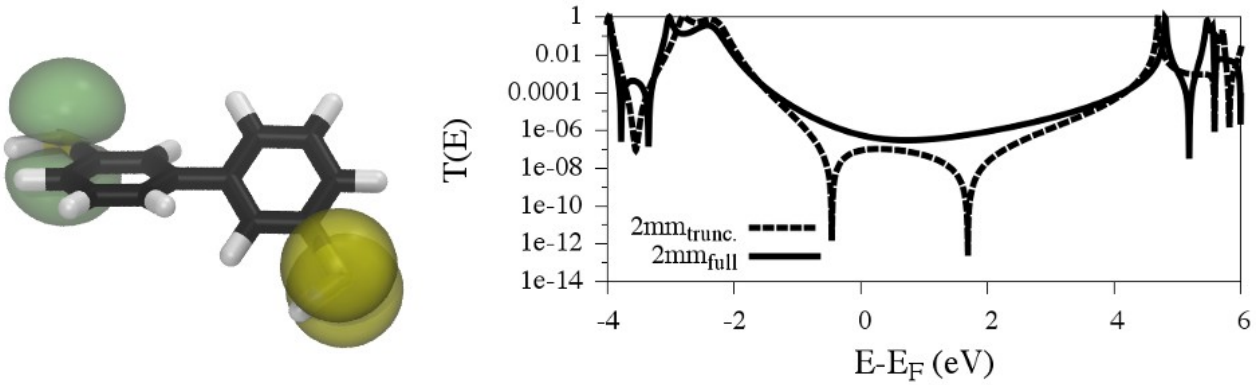

FIG. 3. Left: Representation of the **S2mm** molecule showing the two $2p_z$ orbitals connected to the electrodes. Right: Transmission coefficient obtained using DFT. Two cases are represented: the full DFT Hamiltonian is used (plain line) and the interactions between the two phenyls are limited the coupling between the two connecting atoms (dashed line). The latter clearly shows a sharp interference pattern.

S.6. Variation of the couplings with rotation of the bridge around the C_2 axis in 2pp

As mentioned in the manuscript the symmetry argument exposed in 2.2.4 does not depend on the rotation angle between the different fragments. Fig. 4 shows the individual contributions to the effective coupling between the HOMOs of SNS and PDI in 2pp given by:

$$J_{eff,B_i} = \frac{V_{IB_i} V_{B_i F}}{H_{B_i B_i} - E} \qquad (2)$$

where B_i is the HOMO-2, HOMO-1 and HOMO of the bridge. The bridge was then rotated from 0 to 180° around the C2 axis of the DBA complex. As clearly seen on this

picture the contribution of the HOMO is always null for the symmetry reason exposed in the main text. Similarly, the contribution of the HOMO-1 and HOMO-2 are always opposite to each other regardless of the rotation angle of the bridge.

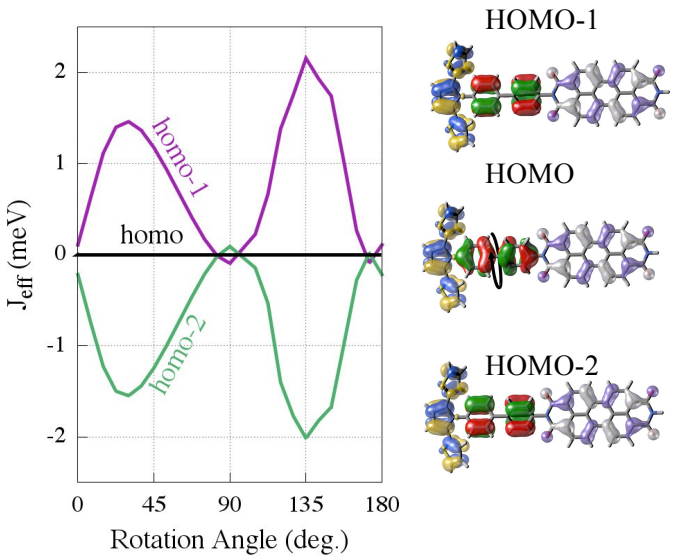

FIG. 4. Variation of selected contributions to the effective coupling for a rotation of the bridge around the C_2 axis.

S.7. Orbital symmetry and pathway selections for 2mm and 2mp

Fig. 5 presents a similar analysis to the one shown in Fig. 10 of the main text but for **2mm** and **2mp**. We focus here on hole transfer, as electron transfer is dominated by a direct transfer from the bridge to the PDI (see main text for details). In the case of **2mp**, SNS does not share the C_2 axis with the bridge and the PDI. Hence, its molecular orbitals are neither symmetric nor antisymmetric with respect to a rotation around this axis. As a consequence, they are coupled with both symmetric and antisymmetric orbitals of the bridge. However, because PDI still shares the C_2 axis with the bridge the same symmetry restrictions as for **2pp** apply here. Consequently, the effective coupling for hole transfer in **2mp** remains low as seen in Fig. 9c of the main text. In **2mm**, neither SNS nor PDI is symmetric around the C_2 axis. Therefore, the HOMO of PDI and of SNS is now coupled to all orbitals of the bridge, opening many additional pathways compared to **2pp** and

2mp. We therefore obtain a relatively large coupling for **2mm** as shown in Fig. 9c of the main text.

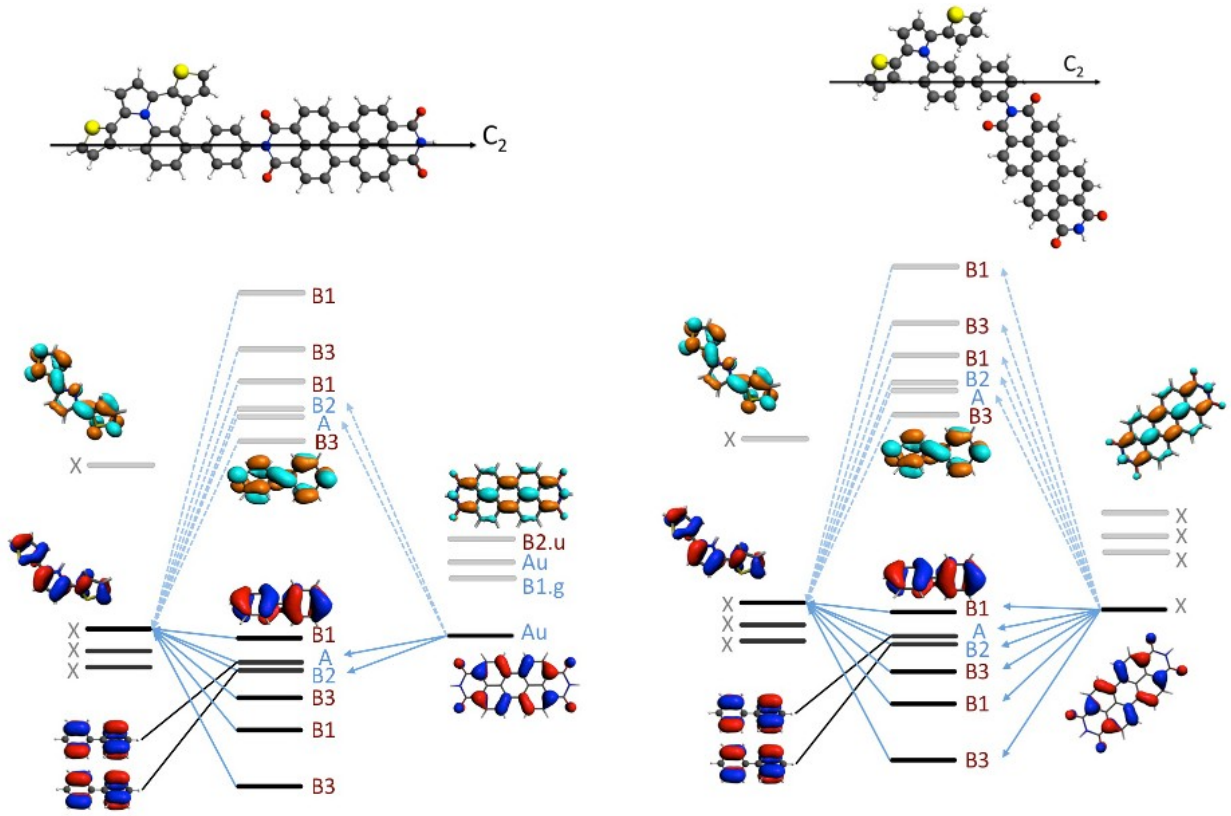

FIG. 5. Illustration of the available pathways for hole transfer along **2mp** (left) and **2mm** (right).

S.8. References

(1) Tarkuc, S.; Sahmetlioglu, E.; Tanyeli, C.; Akhmedov, I. M.; Toppare, L. Electrochim Acta 2006, 51, 5412.

(2) Kaiser, H.; Lindner, J.; Langhals, H. Chem Ber 1991, 124, 529.

(3) Rajaram, S.; Armstrong, P. B.; Kim, B. J.; Frechet, J. M. J. Chem Mater 2009, 21, 1775.

(4) Gorczak, N.; Tarkuc, S.; Renaud, N.; Houtepen, A. J.; Eelkema, R.; Siebbeles, L. D.; Grozema, F. C. J Phys Chem A 2014, 118, 3891.

(5) Kim, K. S.; Kang, M. S.; Ma, H.; Jen, A. K. Y. Chem Mater 2004, 16, 5058.

(6) Snellenburg, J. J.; Laptenok, S. P.; Seger, R.; Mullen, K. M.; van Stokkum, I. H. M. J Stat Softw 2012, 49, 1.

(7) Mullen, K. M.; van Stokkum, I. H. M. J Stat Softw 2007, 18.

(8) van Stokkum, I. H. M.; Larsen, D. S.; van Grondelle, R. Bba-Bioenergetics 2004, 1657, 82.